

Statistical Analysis and Optimization of the MFA Protecting Private Keys

Mahafujul Alam Julie B. Heynssens Bertrand Francis Cambou

School of Informatics, Computing and Cyber Systems, Northern Arizona University,
Flagstaff, AZ 86011, USA

ma3755@nau.edu Julie.Heynssens@nau.edu Bertrand.Cambou@nau.edu

© 2026 IEEE. A two-page version of this paper was published in the 2026 IEEE 23rd Consumer Communications & Networking Conference (CCNC).

DOI: [10.1109/CCNC65079.2026.11366526](https://doi.org/10.1109/CCNC65079.2026.11366526)

Abstract

In the current information age, asymmetrical cryptography is widely used to protect information and financial transactions such as cryptocurrencies. The loss of private keys can have catastrophic consequences; therefore, effective MFA schemes are needed. In this paper, we focus on generating ephemeral keys to protect private keys. We propose a novel bit-truncation method in which the most significant bits (MSBs) of response values derived from facial features in a template-less biometric scheme are removed, significantly improving both accuracy and security. A statistical analysis is presented to optimize an MFA comprising at least three factors: template-less biometrics, an SRAM PUF-based token, and passwords. The results show a reduction in both false-reject and false-acceptance rates, and the generation of error-free ephemeral keys.

Keywords: Zero-knowledge MFA, template-less biometrics, bit-chopping technique, SRAM PUF, ephemeral key generation, private key protection.

1. Introduction

Asymmetric cryptography has been successfully implemented in a wide range of applications vital to the information age, such as cryptocurrencies, secure mail, public key infrastructure, and credit card protection. In distributed cryptocurrency applications, private keys are used to sign all transactions, while public keys are required to verify them. To strengthen this process, Multi-Factor Authentication (MFA) schemes have been proposed to protect private keys with ephemeral keys [1], with the objective of operating in secure zero-trust distributed environments while also delivering zero-knowledge MFA. Here, the term zero-knowledge MFA is defined as an authentication method in which all factors are tested concurrently, thereby preventing serial attacks against individual factors. The development of such a protection scheme is considerably more demanding than conventional MFA schemes, which typically deliver only go/no-go authentication. In contrast, the ephemeral keys generated in our scheme cannot contain a single erroneous bit, and any change in one factor must invalidate

the transaction.

In this work, we propose a bit-chopping technique applied to template-less biometrics. By removing the most significant bits (MSBs) from distance measurements between facial landmarks and challenge points, coarse variations that lead to false acceptances are eliminated, while subject-specific detail is retained. We conduct a statistical analysis of this scheme by varying ADC precision and the number of chopped MSBs, evaluating its impact on false-acceptance, false-reject, and bit-error rates.

We further analyze an SRAM-PUF [2, 3]-based token, focusing on the number of enrollment cycles required to identify unstable cells. The objective is to determine the optimal power-on-off cycle count that minimizes bit errors while keeping the enrollment process efficient. Together, the optimized biometric scheme with MSB bit-chopping and the SRAM-PUF scheme form the basis of a zero-knowledge MFA protocol that generates stable, error-free ephemeral keys for protecting the private keys.

2. Related Work

In Challenge-Response Pair (CRP) Mechanisms and Multi-Factor Authentication Schemes to Protect Private Keys [1], a scheme utilizing a CRP mechanism to generate ephemeral keys for protecting private keys in distributed networks is presented. The scheme incorporates a template-less biometric, an SRAM PUF, and a digital file, combined to generate a cryptotable. This cryptotable can then be challenged to produce responses, from which cryptographic ephemeral keys are derived. The uniqueness of this approach lies in the ability to generate an effectively infinite number of keys on demand.

The work further extended this idea by using the generated keys as seeds for the public key generation part of the CRYSTALS-Dilithium (ML-DSA) [4] digital signature protocol, as well as to generate ephemeral keys that protect the private key produced by the CRYSTALS-Dilithium digital signature scheme. Through the analysis, the authors presented the distribution of 0, 1, and X generated from each reference factor, as well as from the combined factors, i.e., cryptotable. In addition, they applied the Response-Based Cryptographic (RBC) scheme [5] to evaluate key error rates under different fragmentation levels. In testing, user-specific passwords were employed to demonstrate False Reject Rate (FRR) and False Acceptance Rate (FAR) results across different fragmentation levels, validating the practical use case of the scheme.

In this work, we performed a thorough statistical analysis of the proposed architecture to optimize it for real-time use cases. Specifically, we introduced a novel bit-chopping scheme of MSBs that not only strengthens security but also improves overall accuracy, as reflected in the FAR and FRR results. Unlike the earlier study, our work relies on the same password across all users and the same SRAM PUF-based token, thereby demonstrating the strength of the system in discerning different individuals purely through the template-less biometric. We intentionally excluded the digital file factor, as it consistently produced stable reference tables, a finding already established in the prior work.

Furthermore, in this optimization study, we analyzed the template-less biometric scheme and the SRAM-PUF token separately to identify the most effective configurations. For

the biometric scheme, we investigated the optimal accuracy-bit parameter, defined as the Euclidean distance between a challenge point and a landmark point converted into a binary representation, as well as the chopped-MSB parameter, defined as the truncation of the MSBs from the accuracy-bit. For the SRAM-PUF token, we examined the number of enrollment cycles required in order to determine the minimum cycle count necessary for a reliable enrollment operation.

Beyond these contributions, several prior studies have also explored integrating PUFs with biometrics under different assumptions and system models [6–13]. These schemes generally rely on server-side storage of challenge–response pairs or helper data, assume error-free PUF responses, or require the reuse of server-provisioned secrets. While these approaches highlight the potential of combining PUFs and biometrics, they often suffer from practical limitations such as centralized vulnerabilities, error sensitivity, or efficiency trade-offs. By contrast, our work eliminates server-side storage of CRPs, introduces ephemeral key generation to ensure forward secrecy, and operates within a zero-trust framework with mutual authentication, addressing many of the shortcomings identified in earlier protocols.

3. Methodology

We evaluated 10 SRAM-PUF tokens and 6,000 AI-generated images [14]. The dataset comprises 400 individuals with 25 images each: 10 low-variation moment images and 15 high-variation images. From this, 200 individuals were selected; 100 were used for enrollment and 100 for testing.

For the False Acceptance Rate (FAR), enrollment tables from the 100 enrolled individuals were compared against single frames from the 15 variation images of the other 100, producing 150,000 tests. For the False Reject Rate (FRR), each individual’s reference table was compared with its own 10 variation images, yielding 15,000 tests. FRR experiments were repeated 10 times to match the FAR test count, enabling direct comparison in Figure 2.

For SRAM-PUF evaluation, each device produced 202 binary reads (Figure 3), from which 201 ternary enrollment files were derived. One hundred enrollments per token were selected. In each test, 256 addresses from an enrollment file were compared against subsequent binary reads over 1,000 trials. The procedure was repeated across 100 subsequent reads, and results were averaged per enrollment. Figure 3 shows the average key error per file.

The test script followed two phases: enrollment and ephemeral key generation. Enrollment was executed independently for SRAM-PUF tokens and biometric data, as detailed in Algorithms 1 and 2.

We further analyzed the impact of ADC precision (4–8 bits) and MSB removal (0–4 bits) on the biometric system, and the minimum enrollment time for SRAM-PUFs. Results are shown in Figures 2 and 3.

Finally, we evaluated the combined system. Table 1 summarizes the best-performing configurations, and Figure 4 confirms that the generated keys exhibit no detectable bias. All experiments were conducted on an Intel[®] Core™ i9-9900K CPU @ 3.60 GHz with 32 GB RAM and an NVIDIA RTX 3070 GPU.

3.1. Enrollment Phase

3.1.1. SRAM PUF Token

During the enrollment phase of the SRAM-PUF token, repeated power-cycling of the device yields multiple million-bit SRAM dumps. From these dumps, a password- and RN1-seeded generator deterministically selects 256×256 cell indices. Through repeated cycles, we construct a ternary table $T \in \{0, 1, X\}^{256 \times 256}$.

Each individual read produces a binary table; the final ternary table is obtained by superimposing multiple reads. If a specific cell position consistently retains the same value across all reads, it is considered a stable cell, and its bit value is preserved. Conversely, if flips are observed in sequential reads at a given cell position, that position is marked as X, denoting a flaky cell. The complete process is described in Algorithm 1.

3.1.2. Template-less Biometrics

The enrollment process for template-less biometrics is based on a challenge–response mechanism. Facial landmarks are detected on enrollment frames using Dlib [15]. Randomly generated challenge points are placed on each frame, and Euclidean distances between landmarks and challenge points are computed. These distances form the raw measurements that are transformed into binary responses.

To improve stability, we apply Gray coding and introduce a bit-chopping step: MSBs of each distance measurement are removed before conversion. MSB chopping reduces overlap between biometric responses by filtering out large but uninformative variations, while preserving lower-order bits that encode subject-specific distinctions.

Finally, 64 landmark indices are deterministically selected from a password-derived seed. From multiple frames, the results are superimposed into a 256×256 table: stable positions retain their binary values, while unstable ones are marked as X. In Algorithm 2, we present the step-by-step process that demonstrates how this template-less biometric scheme operates in practice.

3.2. Ephemeral Key Generation

The key generation process for both the server and client follows the same structure; however, unlike the enrollment phase, only a single read is used at this stage. The server transmits the ternary table information to the client along with RN1 and RN2. On the server side, a template-less format combining the SRAM-PUF template-less biometric tables is employed, and the final key is derived using RN2 together with the user password. The client mirrors this procedure by generating binary tables from one-shot reads of the SRAM-PUF token and facial biometric, while incorporating the ternary table received from the server. Using the same RN1, RN2, and password ensures alignment with the server’s process. After constructing its key, the client applies Response-Based Cryptography (RBC) to guarantee consistency with the server’s reconstruction, while the server compares its own generated key against the fragmented, hashed key received from the client, applying RBC error correction [5] to mitigate real-time noise. Through this protocol, both parties converge on an identical key, which can then serve as a secure seed for post-quantum cryptographic schemes or be directly applied for encryption and decryption to protect private keys. To simplify

Algorithm 1 SRAM PUF Table Construction

Input: Cycles N ; serial port P ; password pwd ; $RN1 \in \{0, 1\}^{512}$; PUF size $M = 1,048,576$ bits (= 131,072 bytes); table size $C = 256 \times 256$

Output: $T \in \{0, 1, X\}^{256 \times 256}$

- 1: **Acquire million-bit dumps:**
- 2: **for** $k \leftarrow 1$ **to** N **do**
- 3: Power on; wait t_{settle} ; open P ; trigger read;
- 4: Read exactly 131,072 bytes \rightarrow bitstring $R^{(k)} \in \{0, 1\}^M$;
- 5: Power off; wait t_{sleep}
- 6: **end for**
- 7: **Derive keyed addresses ($RN1 \parallel \text{password}$):**
- 8: $RN1 \leftarrow$ 512 uniform random bits;
- 9: $pwd_{512} \leftarrow \text{SHA3-512}(pwd)$;
- 10: Byte stream $z \leftarrow \text{SHAKE-256}(RN1 \parallel pwd_{512})$;
- 11: $S \leftarrow \emptyset$;
- 12: **while** $|S| < C$ **do**
- 13: $u \leftarrow$ next uint32 from z ; $s \leftarrow u \bmod M$;
- 14: **if** $s \notin S$ **then**
- 15: insert s into S
- 16: **end if**
- 17: **end while**
- 18: Let $S = [s_0, \dots, s_{C-1}]$ be the ordered list of selected cell indices.
- 19: **Bit stability at selected cells:**
- 20: **for** $i \leftarrow 0$ **to** $C - 1$ **do**
- 21: **if** $R^{(1)}[s_i] = R^{(2)}[s_i] = \dots = R^{(N)}[s_i]$ **then**
- 22: $U[i] \leftarrow R^{(1)}[s_i]$
- 23: **else**
- 24: $U[i] \leftarrow X$
- 25: **end if**
- 26: **end for**
- 27: Generate the Token Table T .

the testing process, both the server and client were executed within the same script. The complete procedure of ephemeral key generation is illustrated in Figure 1.

4. Experimental Evaluation

4.1. Template-less Biometrics Analysis

We tested a total of 15 configurations; however, in Figure 2 we only present the results for accuracy-bit and chopped-MSB configurations of (6,1), (6,2), (7,1), (7,2), (8,1), and (8,2). Our experimental analysis shows that the gap between correct and incorrect individuals increases as the number of distance bits grows, and further increases with a larger number of chopped MSBs. While increasing accuracy-bits and chopped-MSBs has a positive effect on differentiating between users—in other words, reduced FAR—we later observed that it can

Algorithm 2 BioTable Construction

Input: Password pwd ; $RN1 \in \{0, 1\}^{512}$; frames N ; frame size $F = 256$; table size $C = F^2$; accuracy-bits g ; chopped-MSBs m

Output: Ternary BioTable $B \in \{0, 1, X\}^{F \times F}$

- 1: **Face alignment & landmarks:** Obtain aligned face chips of size $F \times F$; detect 68 landmarks per chip; seed RNG with $\text{SHA256}(pwd)$ and select 64 unique landmark indices.
- 2: **Challenge generation:** Derive C pseudorandom challenge coordinates in $[0, F) \times [0, F)$ from $\text{SHAKE-256}(RN1 \parallel \text{SHA3-512}(pwd))$.
- 3: **Per-frame distance features:** For each frame f and challenge q_i , compute Euclidean distances to 64 selected landmarks: $d_i^{(f)} \in \mathbb{R}^{64}$.
- 4: **Quantization to Gray code:** $D_{\max} \leftarrow \sqrt{2} F$;
- 5: **for** each frame f and challenge i **do**
- 6: **for** $j = 1 : 64$ **do**
- 7: $w \leftarrow \lfloor \frac{d_i^{(f)}[j]}{D_{\max}} \cdot 2^g \rfloor$;
- 8: Take g -bit binary of w , chop m MSBs; convert remaining $(g-m)$ bits to Gray code; concatenate over j to get bitarray $R_i^{(f)}$.
- 9: **end for**
- 10: **end for**
- 11: **Multi-frame unanimity** \rightarrow **ternary map:** Initialize $U \in \{0, 1, X\}^C$;
- 12: **for** each bit index $i = 1 : C$ **do**
- 13: **if** all frames agree at bit i **then**
- 14: $U[i] \leftarrow$ unanimous bit
- 15: **else**
- 16: $U[i] \leftarrow X$
- 17: **end if**
- 18: **end for**
- 19: Construct BioTable T .

also raise the FRR. Some overlap between correct and incorrect individuals is visible, which occurs because the protocol is designed for straight-face images and is less tolerant to angle variations. To evaluate these limitations, we performed enrollment primarily on straight-face images and then conducted key generation using the variation bucket of images. Our future goal is to design a protocol that supports 3D facial data, which will eliminate these overlaps and improve robustness.

4.2. SRAM PUF Token Analysis

In Figure 3, we analyze the average key error versus the number of enrollments. As the number of enrollments increases, the average error clearly decreases. This behavior arises from a fundamental property of SRAM PUFs: with more reads, unstable cells can be more effectively identified and flagged. However, the practical limit of enrollment must be considered, since increasing enrollment time also increases the overall cost of the process. Our experiments show that 20 enrollments are sufficient to generate keys with limited error, and

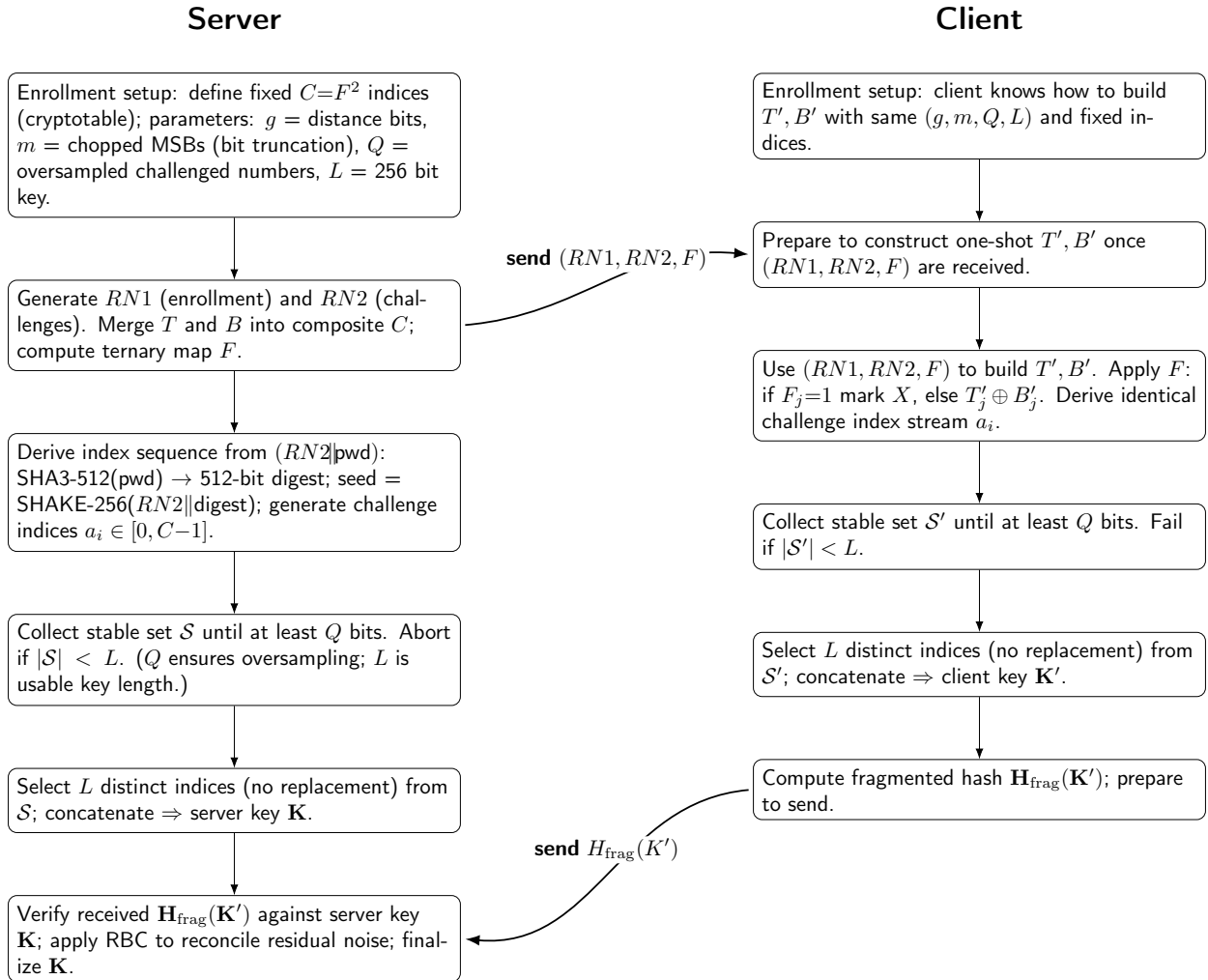


Figure 1: Protocol diagram for ephemeral key generation.

the RBC error correction scheme can reliably handle this level of noise.

4.3. Key Bias Test

To evaluate the balance between zeros and ones in the generated ephemeral keys, we conducted exact binomial tests under the null hypothesis of an unbiased bitstream ($p(1) = 0.5$), as the results show in Figure 4. For the client pool ($n = 115,200$), the observed proportion of ones was $\hat{p} = 0.4998$ with a 95% confidence interval of $[0.4969, 0.5027]$, yielding a non-significant result ($p = 0.9085$). Similarly, the server pool ($n = 115,200$) produced $\hat{p} = 0.4999$, 95% CI $[0.4970, 0.5027]$, with $p = 0.9225$. In both cases, the confidence intervals tightly bound 0.5, and the high p -values indicate no evidence of systematic bias in the relative frequencies of zeros and ones.

4.4. Overall Result

As shown in the top five configuration results in Table 1, our technology demonstrates promising potential, achieving 0% FAR and 0% FRR. This test was performed using a

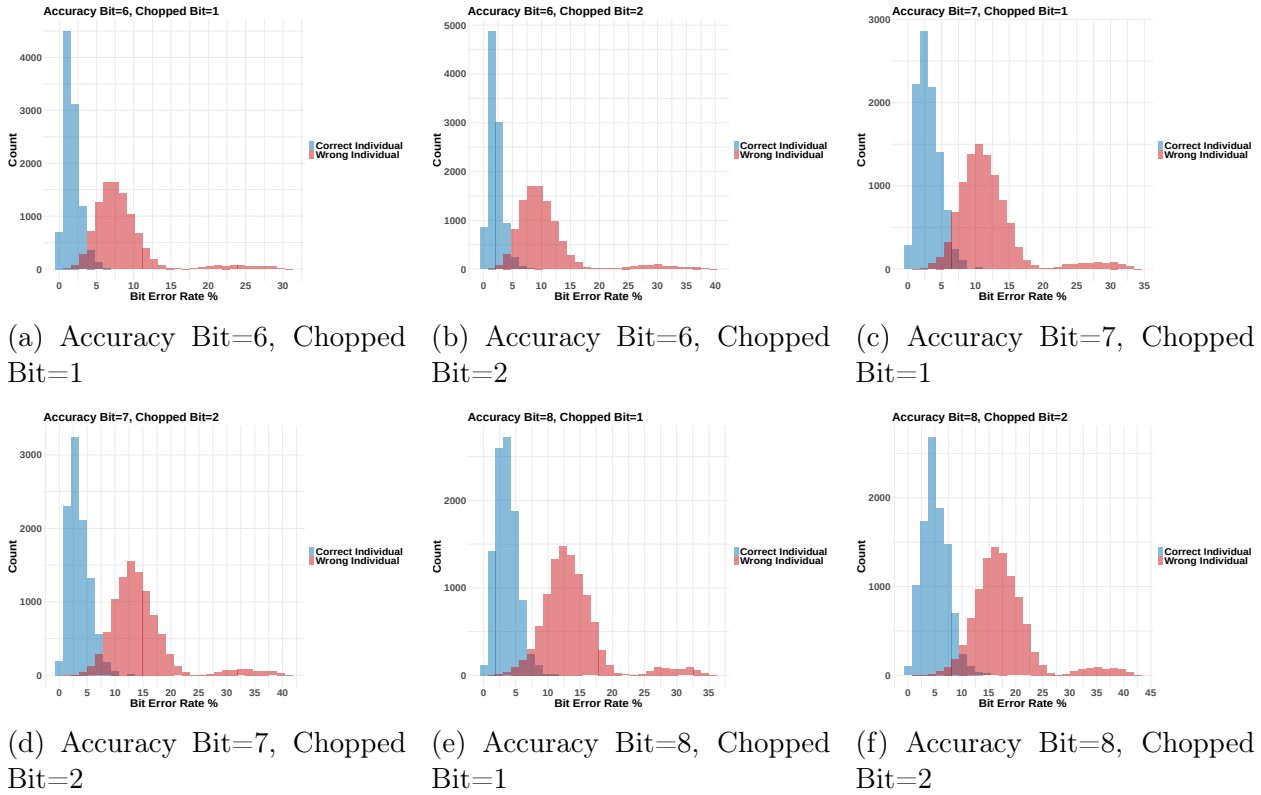


Figure 2: Comparison of histograms for different configurations for template-less biometrics based on (Distance bits, Chopped MSB).

random sampling of $n = 30$ from the dataset. For this evaluation, we assumed that all users share the same password and the same token, with enrollment performed over 40 cycles. On average, each enrollment cycle takes about 5 seconds, resulting in a total enrollment time of less than 3.5 minutes. However, we later determined that 20 enrollment cycles are sufficient, as the number of fragmentations in RBC can be increased to tolerate one or two additional bit flips caused by the reduced number of enrollments.

Table 1: Top 5 configurations with lowest error rates.

Frag. Level	Accuracy Bits	Chopped MSB	FAR (%)	FRR (%)
1	7	1	0.0	0.0
1	7	2	0.0	0.0
2	7	2	0.0	0.0
1	6	2	0.0	1.7
4	7	2	3.3	0.0

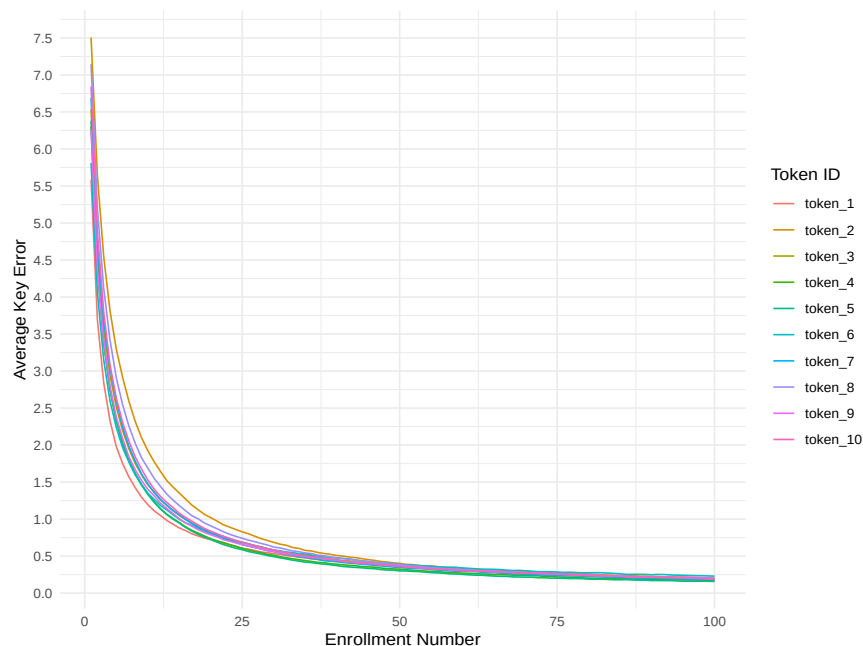


Figure 3: Number of key errors reduces as we increase the number of enrollments for SRAM PUF Token.

5. Security Analysis

5.1. Resistance to Sequential Attacks

Since the authentication template is a combination of template-less biometrics and the SRAM-PUF token, sequential attacks cannot be mounted successfully. The dynamic and fused nature of the template prevents adversaries from exploiting repeated authentication attempts.

5.2. Resistance to Insider Attacks

The stored template is one-way and unlinkable. Even in the event of insider access, the protected credentials do not reveal usable information about the user’s biometric features or PUF responses.

5.3. Resistance to Man-in-the-Middle Attacks

Although an adversary may intercept random nonces ($RN1$, $RN2$) during transmission, these values alone are insufficient to reconstruct the authentication key. Without access to the actual PUF responses and facial biometric data, the intercepted information has no utility.

5.4. Resistance to Modeling Attacks

Modeling attacks are ineffective because the system does not rely on static challenge–response pairs. Instead, it generates a template-less cryptotable, making it infeasible for an attacker to reconstruct or predict the key through machine learning or statistical modeling.

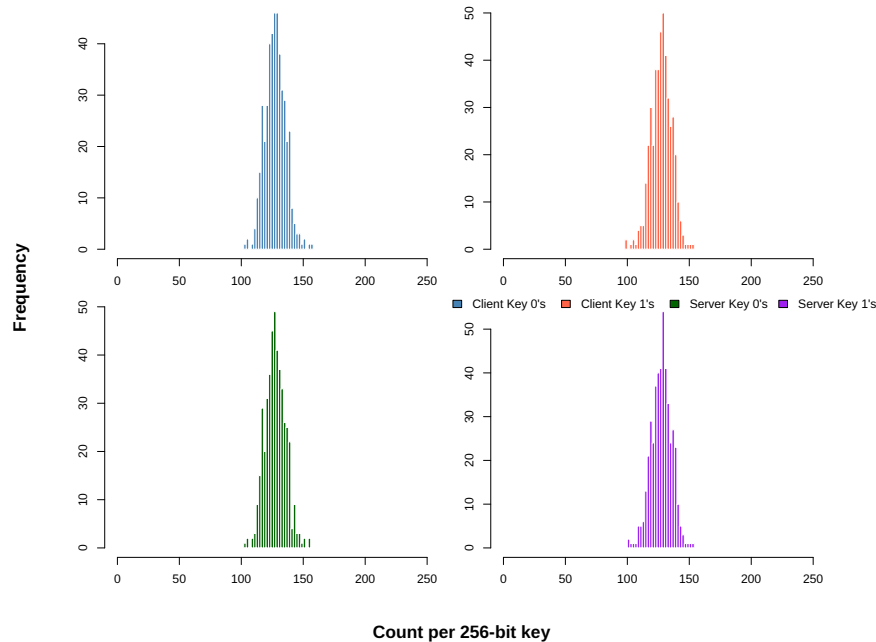


Figure 4: No bias in the generated key.

5.5. Mathematical One-wayness of the Cryptotable

Theorem 1. Let f be the cellwise merge operator defined by

$$D_{ij} = \begin{cases} X, & \text{if } A_{ij} = X \text{ or } B_{ij} = X, \\ A_{ij} \oplus B_{ij} \oplus C_{ij}, & \text{if } A_{ij}, B_{ij} \in \{0, 1\}, \end{cases}$$

with $A, B \in \{0, 1, X\}^{n \times n}$ and $C \in \{0, 1\}^{n \times n}$. Then f is not injective.

Proof 1 (Counting Argument). Consider a cell (i, j) with $D_{ij} \in \{0, 1\}$. The triple (A_{ij}, B_{ij}, C_{ij}) must satisfy the linear constraint $A_{ij} \oplus B_{ij} \oplus C_{ij} = D_{ij}$. This is one parity equation over three binary variables, leaving two degrees of freedom. Thus there are exactly 4 valid preimages for each such output cell. If m cells of D take binary values, the total number of preimages is 4^m . Cells with $D_{ij} = X$ admit even more preimages, since at least one of A_{ij} or B_{ij} can be freely chosen as X . Hence the map f is highly many-to-one. \square

Proof 2 (Explicit Collision). Fix a cell (i, j) such that $D_{ij} \in \{0, 1\}$. Suppose $(A_{ij}, B_{ij}, C_{ij}) = (0, 0, C_{ij})$ yields $D_{ij} = C_{ij}$. Then the alternative assignment $(A_{ij}, B_{ij}, C_{ij}) = (1, 1, C_{ij})$ also yields the same output, since $1 \oplus 1 = 0$ and thus $1 \oplus 1 \oplus C_{ij} = C_{ij}$. Therefore, by modifying (A, B) at a single cell from $(0, 0)$ to $(1, 1)$ (keeping C fixed), one obtains a distinct input triple with identical output D . This exhibits a collision and proves that f is not injective. \square

6. Future Work

This work establishes the groundwork for a practical, application-level zero-knowledge MFA technology to protect private keys in a distributed network. There remain several avenues for

improvement. One direction is the addition of a sensor-based PUF factor, which is currently under development and will later be embedded in wearable devices. Another direction is the design of a challenge–response protocol using 3D biometrics to enhance the robustness of the current 2D-based system. Furthermore, conducting case studies—such as the protection of medical records or the integration with blockchain technology—could demonstrate the applicability of this approach and open new research directions. Finally, a thorough security analysis of the proposed architecture is currently underway.

7. Conclusion

This work demonstrates that the proposed bit-chopping of MSBs significantly improves both the accuracy and security of the architecture. Statistical analysis enabled the optimization of template-less biometry and SRAM-PUF-based key generation. In the template-less biometric scheme, insufficient distance accuracy leads to high false-acceptance rates, while excessive accuracy increases false-reject rates. Analysis of 4–8 ADC precision bits with 0–4 MSBs removed indicates that 6–7 bits of precision with 1–2 MSBs removed achieve the best balance. Furthermore, eliminating MSBs reduces false acceptances without substantially affecting legitimate users.

For the SRAM-PUF scheme, approximately 20 power-off/power-on enrollment cycles are sufficient to identify and eliminate unstable cells. Beyond this threshold, additional cycles yield minimal improvement in bit error rates, allowing the enrollment process to remain short and efficient.

Future work will focus on incorporating additional authentication factors and further strengthening the security of the protocol.

References

- [1] B. F. Cambou and M. Alam, “Challenge–Response Pair Mechanisms and Multi-Factor Authentication Schemes to Protect Private Keys,” *Applied Sciences*, vol. 15, no. 6, p. 3089, 2025.
- [2] B. Gassend, D. Clarke, M. van Dijk, and S. Devadas, “Silicon physical random functions,” in *Proceedings of the 9th ACM Conference on Computer and Communications Security, CCS’02*, pp. 148–160, Association for Computing Machinery, 2002.
- [3] C. Herder, M.-D. Yu, F. Koushanfar, and S. Devadas, “Physical Unclonable Functions and Applications: A tutorial,” *Proceedings of the IEEE*, vol. 102, no. 8, pp. 1126–1141, 2014.
- [4] S. Bai, L. Ducas, E. Kiltz, T. Lepoint, V. Lyubashevsky, P. Schwabe, G. Seiler, and D. Stehlé, “CRYSTALS-Dilithium: A lattice-based digital signature scheme,” *IACR Transactions on Cryptographic Hardware and Embedded Systems*, 2021.
- [5] B. Cambou, M. Mohammadi, C. Philabaum, and D. Boohar, “Statistical Analysis to Optimize the Generation of Cryptographic Keys from Physical Unclonable Functions,” in *Intelligent Computing* (K. Arai, S. Kapoor, and R. Bhatia, eds.), pp. 302–321, Springer International Publishing, 2020.

- [6] Y. Zheng, W. Liu, C. Gu, and C.-H. Chang, “PUF-based mutual authentication and key exchange protocol for peer-to-peer IoT applications,” *IEEE Transactions on Dependable and Secure Computing*, vol. 20, no. 4, pp. 3299–3316, 2023.
- [7] Y. Zheng, Y. Cao, and C.-H. Chang, “UDhashing: Physical unclonable function-based user-device hash for endpoint authentication,” *IEEE Transactions on Industrial Electronics*, vol. 66, no. 12, pp. 9559–9570, 2019.
- [8] Y. Zheng and C.-H. Chang, “Secure mutual authentication and key-exchange protocol between PUF-embedded IoT endpoints,” in *2021 IEEE International Symposium on Circuits and Systems (ISCAS)*, pp. 1–5, 2021.
- [9] J. R. Wallrabenstein, “Practical and secure IoT device authentication using physical unclonable functions,” in *2016 IEEE 4th International Conference on Future Internet of Things and Cloud (FiCloud)*, pp. 99–106, 2016.
- [10] M. N. Aman, K. C. Chua, and B. Sikdar, “Mutual authentication in IoT systems using physical unclonable functions,” *IEEE Internet of Things Journal*, vol. 4, no. 5, pp. 1327–1340, 2017.
- [11] T. Idriss and M. Bayoumi, “Lightweight highly secure PUF protocol for mutual authentication and secret message exchange,” in *2017 IEEE International Conference on RFID Technology & Application (RFID-TA)*, pp. 214–219, 2017.
- [12] Y. Zheng, Y. Cao, and C.-H. Chang, “Facial bihashing based user-device physical unclonable function for bring your own device security,” in *2018 IEEE International Conference on Consumer Electronics (ICCE)*, pp. 1–6, 2018.
- [13] B. Zahednejad and C.-z. Gao, “A secure and efficient AKE scheme for IoT devices using PUF and cancellable biometrics,” *Internet of Things*, vol. 24, p. 100937, 2023.
- [14] Generated Photos, “Generated photos: AI generated faces.” <https://generated.photos/>, 2025. Accessed: 2025-08-29.
- [15] D. E. King, “Dlib-ml: A machine learning toolkit,” *Journal of Machine Learning Research*, vol. 10, pp. 1755–1758, 2009.